SYNTHESIS, STRUCTURAL AND MAGNETIC PROPERTIES OF TM$^{2+}_2$[Mo^{IV}(CN)$_8$]·nH$_2$O

ZUZANA MITRÓOVÁ, MARIÁN MIHALIK, ANTON ZENTKO, MÓNIKA BOKOR*, KATALIN KAMARÁS*,
VIKTOR KAVEČANSKÝ, JOZEF KOVÁČ, KORNEL CSACH, JARMILA TRPČEVSKÁ**

Institute of Experimental Physics SAS, Watsonova 47, 043 53 Košice, Slovakia
*Research Institute for Solid State Physics and Optics of the Hungarian Academy of Science,
P.O. Box 49, H-1525 Budapest, Hungary
**Technical University of Košice, Letná 9, 042 00 Košice, Slovakia

E-mail: mitro@saske.sk

Octacyanomolybdates (OCMs) TM$^{2+}_2$[Mo(CN)$_8$]·nH$_2$O, where TM is Mn, Fe, Co, Ni, Cu were synthesised and characterised by IR spectroscopy and UV-VIS spectroscopy. The UV-VIS spectrum showed the intervalence charge transfer (IVCT) band between Mo^{IV}-CN-Cu^{II} and Mo^V-CN-Cu^I around 510 nm. Studied OCMs adopt tetragonal crystal structure. The ^{1}H NMR signals reflect the magnetic moment of the TM^{2+} ions (μ_P). The decay rates of free induction decay (FID) signals increase as μ_P and the applied static rf -field increases. The spin - lattice relaxation times at 27.7 MHz vary from 0.0187 ms (Mn) up to 0.45 ms (Cu). Magnetization measurements indicate long-range magnetic ordering of Mn- and Co- OCMs with the Curie temperature T_c = 4 K. The remaining OCMs (TM is Fe, Ni, Cu) are paramagnetic down to T=1.9 K.

INTRODUCTION

During the past years interest in the cyanocomplexes was revived due to the fact that they are building blocks of magnetic clusters and networks [1-7]. One of the great advantages of these materials is that novel functions like control of the magnetic properties via external stimuli, can be incorporated through a proper design of their electronic structure. It has been reported the examples of magnetic ordering temperature (T_C) control, via electrochemical stimuli [8] on chromium cyanide thin film and optical stimuli [9], where first example of a photo-induced reversible change between a paramagnet and a ferrimagnet was described in a Prussian blue analog, K$_{0.2}$Co$_{1.4}$[Fe(CN)$_6$]·6.9H$_2$O. Similar photo-induced change of magnetization can be observed on other types of cyanometallates; photo-magnetic effect was investigated on Cu$_2$[Mo(CN)$_8$]·8H$_2$O [10]. Since no complete study of OCMs has been reported we prepared and studied physical properties of TM$^{2+}_2$[Mo(CN)$_8$]·nH$_2$O, where TM is Mn, Fe, Co, Ni and Cu.

EXPERIMENTAL

Sample preparation

Potassium octacyanomolybdate (IV) was prepared by the method of Brauer [11]. The divalent cation salts (TMCl$_2$) were of p.a. grade. All the OCMs were pre-

pared by the same technique; by slow mixing of saturated aqueous solutions of K$_4$[Mo(CN)$_8$]·2H$_2$O (22-25 ml) with the aqueous solution (c = 0.5 M) of TMCl$_2$ (except Fe^{2+}, where FeSO$_4$ was used) at room temperature following the formal equation:

2TMCl$_2$ (aq) + K$_4$[Mo(CN)$_8$] (aq) → TM$_2$[Mo(CN)$_8$]·
·nH$_2$O (s) + 4KCl (aq)

In all cases, except Mn^{2+}, process of precipitation started immediately. In the case of Mn$_2$[Mo(CN)$_8$]·8H$_2$O the process started in about 10 min. The solids were collected by filtration, washed two times with 10 ml of water and dried above KOH. The typical distribution of well crystalline particles for the Mn$_2$[Mo(CN)$_8$]·8H$_2$O sample can be seen from scanning electron micrograph (figure 1). The remaining OCMs crystallize worse, for example Cu$_2$[Mo(CN)$_8$]·7H$_2$O (also shown in figure1).

Instruments

Infrared spectra were observed by using FT-IR spectrometer Avatar 330 in the range from 400 to 4000 cm^{-1} using KBr tablets. UV-VIS spectra were also measured in pressed KBr pellets by an Ocean Optics SD 1000 fiber optic spectrometer (low resolution), and a JASCO V-550 dual-channel spectrophotometer (high resolu-

tion) using pure KBr as a reference. The number of water molecules was determined from thermogravimetric analysis using a SETARAM TG/DTA 9L equipment. The TG curves were obtained by heating from room temperature up to 620°C at the heating rate 10 K/min under Ar-atmosphere. The NMR measurements and data acquisition were accomplished by a Bruker SXP 4-100 pulse spectrometer at room temperature. Diffraction patterns were taken using $Co_{K\alpha}$ X ray radiation ($\lambda = 1.7902$ Å, angular range from 10° to 120° 2θ, HZG4/A) and $Cu_{K\alpha}$ X-ray radiation ($\lambda = 1.54184$ Å, from 5° to 100° 2θ, PANalytical X'Pert). The crystal structure refinement was performed using the software package FullProf [12]. Free induction decay (FID) signals were detected and spin-lattice relaxation time (T_1) was measured at $\nu_0 \equiv \omega_0/2\pi = 27.694$ and 82.556 MHz. T_1 mea-surements were made with the inversion-recovery method. Magnetization measurements were performed using a SQUID magnetometer (Quantum Design) and a sample vibrating magnetometer in the temperature range 2-200 K or 4.2 K < T < 290 K and in the magnetic fields up to 5 T.

RESULTS AND DISCUSSION

Infrared spectroscopy

The analysis of IR spectra showed that the spectrum of $K_4[Mo(CN)_8]\cdot2H_2O$ agrees well with that reported by Kettle and Parish [13] for dodecahedral D_{2d} structure of $[Mo(CN)_8]$ unit [14]. Four strong bands are seen at 2102, 2123, 2127, and 2135 cm^{-1} (figure 3). In the case of OCMs the geometry of $[Mo(CN)_8]$ unit is changed from D_{2d} one in the starting $K_4[Mo(CN)_8]\cdot2H_2O$ to square antiprismatic D_{4d} (figure 2) [18, 20, 21].

The IR spectra of OCMs (summarized in table 1) shows a single strong $\nu_{(CN)}$ peak about 60 cm^{-1} wide at half height. (See the case of $Ni_2[Mo(CN)_8]\cdot8H_2O$ in figure 3. for example.)

Table 1. Summarization of infrared measurements of $TM_2[Mo(CN)_8]\cdot nH_2O$ in the cyanide stretching region.

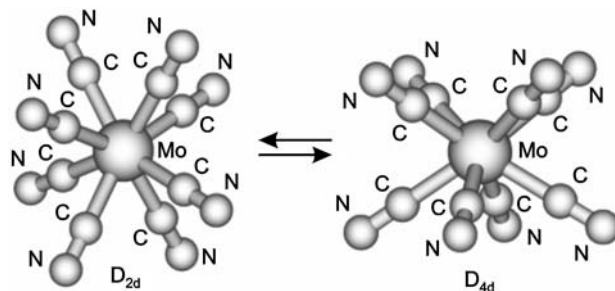| TM	Mn	Fe	Co	Ni	Cu
$\nu_{(CN)}$ (cm^{-1})	2133	2137	2144	2152	2164

Figure 2. Dodecahedral D_{2d} and square antiprismatic D_{4d} geometries of the OCMs [15].
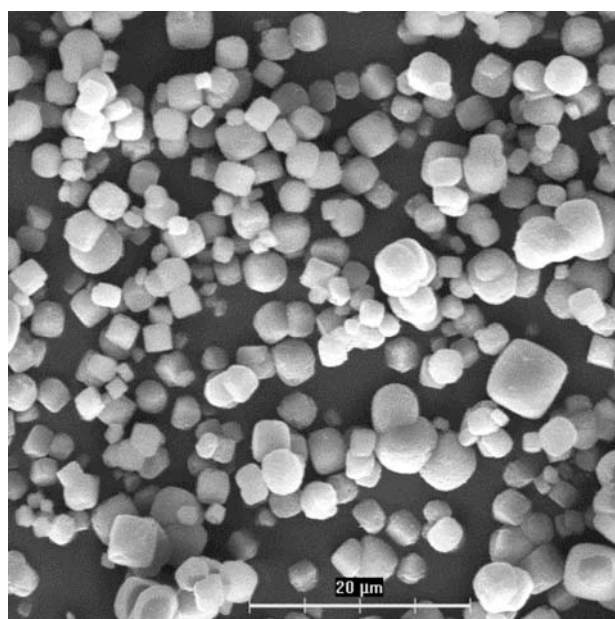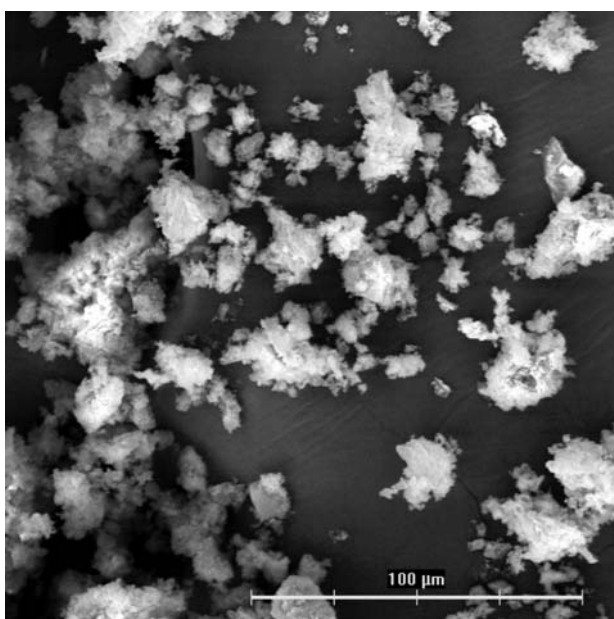

Figure 1. Scanning electron micrographs of $Cu_2[Mo(CN)_8]\cdot7H_2O$ (left) and $Mn_2[Mo(CN)_8]\cdot8H_2O$ (right) powder particles.

Our results correspond with recently published results in [16]. The values of $\nu_{(CN)}$ for all OCMs are shifted to higher frequencies than those of $K_4[Mo(CN)_8]\cdot 2H_2O$ that indicate the bridging nature of the cyano groups –TM–NC–Mo–CN–TM–.

UV-VIS spectroscopy

UV-VIS spectra of OCMs, which include Mn, Fe, Co, Ni are a simple superposition of the bands of their components. Such is thecase of $Mn_2[Mo(CN)_8]\cdot 8H_2O$ in the inset in figure 4). In the case of $Cu_2[Mo(CN)_8]\cdot 7H_2O$ we can see a suplementary band in the visible region at arround 510 nm (figure 4). This absorption band correspond to the optical absorption spectra of ion pair $Cu^{II}/[Mo^{IV}(CN)_8]^{4-}$ in the solution. By excitation of this band the intermolecular electron transfer process produce the metastabile valence isomer $Cu^{I}/[Mo^{V}(CN)_8]^{3-}$ [17]. This same photo-induced electron transfer occurs in the corresponding solid phase and $Cu^{II}_2[Mo^{IV}(CN)_8]$ will be changed by irradiation to $Cu^{II}Cu^{I}[Mo^{V}(CN)_8]$ [5].

X -ray diffraction

A set of powder samples $TM_2[Mo(CN)_8]\cdot nH_2O$ (TM is Mn, Fe, Co Ni, and Cu) was investigated by X-ray diffraction. The crystal structure of $Fe_2[Mo(CN)_8]\cdot 8H_2O$ was refined in accordance with the structural model described by Sra et al. [18]. The obtained results are summarized in figure 5 and table 2. The structural model suggested by Willemin et al. [20] was used for the crystal structure refinement of $Mn_2[Mo(CN)_8]\cdot 8H_2O$ phase. The structure is tetragonal (space group *I4/mcm*), refined values of lattice parameters are a = b = 11.679 (4) Å, c = 13.205 (6) Å. The crystal structure of $Ni_2[Mo(CN)_8]\cdot 8H_2O$ phase has not been yet determined. Indexing procedure confirmed for the phase tetragonal symmetry, too. The structureless profile matching fit gave refined values of lattice parameters a = b = 11.555 (4) Å and c = 14.044 (6) Å. $Co_2[Mo(CN)_8]\cdot 8H_2O$ phase was reported to crystallize in the tetragonal system (*I4/m*) [20, 21]. Unfortunately in our case the indexing procedure failed for TM is Co and Cu. However, for $Cu_2[Mo(CN)_8]\cdot 8H_2O$ it was probably caused by the low

Table 2. Refined values of selected structural parameters of $Fe_2[Mo(CN)_8]\cdot 8H_2O$.

| Tetragonal			x	y	z	Uiso	Occ
Space group	*I 4 2 2*	Fe	0.1960(3)	0.3041(3)	0.25000	0.01607	1.00000
a (Å)	11.80321 (15)	Mo	0.00000	0.00000	0.00000	0.01189	1.00000
b (Å)	11.80321 (15)	C1	0.059(4)	0.153(3)	0.406(3)	0.03163	1.00000
c (Å)	13.1008 (2)	N1	0.0867(18)	0.224(2)	0.372(3)	0.02531	1.00000
α	90.0	C2	0.074(4)	0.126(3)	0.081(2)	0.03996	1.00000
β	90.0	N2	0.1356(19)	0.204(2)	0.142(2)	0.02995	1.00000
γ	90.0	O1	0.2885(19)	0.1377(18)	0.267(3)	0.02429	0.50000
Cell volume (Å)³	1825.15 (5)	O2	0.1015(18)	0.4536(17)	0.274(2)	0.02663	0.50000
		O3	0.114(2)	0.408(3)	0.5564(11)	0.09622	1.00000
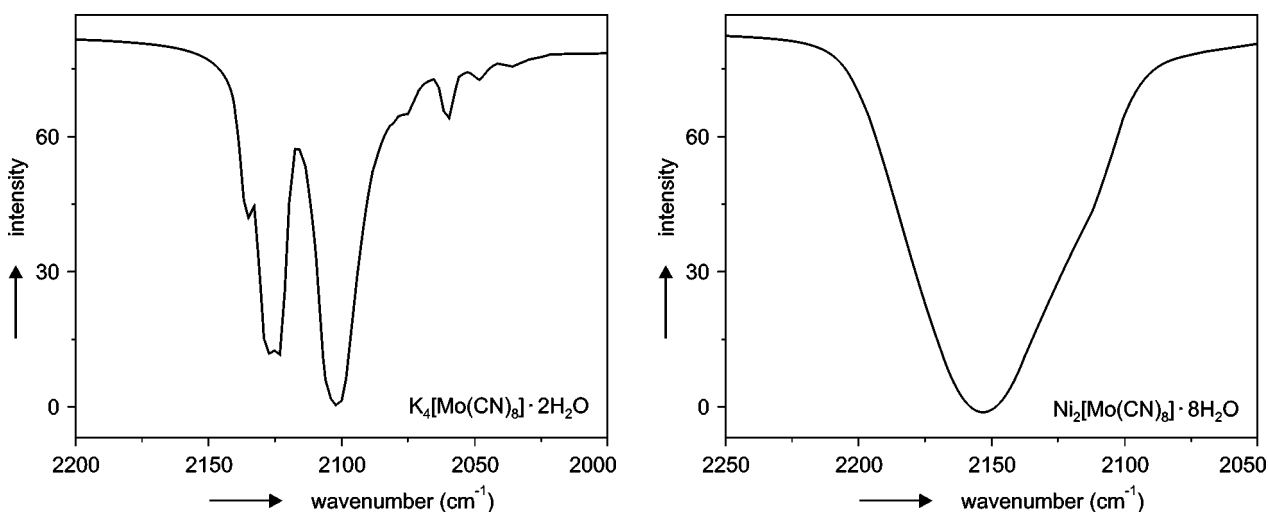
Figure 3. Infrared spectra of $K_4[Mo(CN)_8]\cdot 2H_2O$ and $Ni_2[Mo(CN)_8]\cdot 8H_2O$.

quality of powder diffraction pattern due to significant contribution of poor crystallized component. Similarly Cu-OCM was reported as poorly crystallized sample [19, 23] unlike $Cu_2[W(CN)_8]\cdot 8H_2O$ which crystallizes well in the orthorhombic system (space group *Pbcn*).

NMR spectroscopy

The ^1H nuclei in the water molecules served as local probes in the NMR experiments. The FID signals showed a behaviour peculiar to paramagnetic samples. They decayed more rapidly in a higher applied static field $B_0 = \omega_0/\gamma_{1H}$ (figure 6b). Their decay rates described by an effective spin-spin relaxation time (T_{2eff}) increase as the magnetic moment of the transition-metal ions (table 3).

The amplitude of the FID signal at $t = 0$ is proportional to the number of ^1H nuclei in the sample. This makes possible to determine the amount of water i.e. the molar ratio n. Unfortunately the resonance frequency of the protons near to the first-row transition metal ions is shifted by the local magnetic moments so far from the applied frequency that the signal of these protons is not detected. This means that a part of the water content is unseen and the water concentration cannot be determined. Only a lower limit for n could be calculated in an ideal case. The FID signal at $0 > t > (10-20)$ μs is concealed by the dead time of the spectrometer. There is no theoretical model for the exact shape of the FID measured in this kind of samples. The extrapolation to $t = 0$ has not been made because of a big error of the extrapolated value resulting from a fit with a trial function.

The recovery of the magnetization in the spin-lattice relaxation experiments was single-exponential at $v_0 = 27.694$ MHz and it could be described by a sum of two exponentials at $v_0 = 82.556$ MHz (table 3). $Mn_2[Mo(CN)_8]\cdot 8H_2O$ showed two-exponential relaxation at the lower frequency also ($93.4\% \times exp[t/(0.0187$ ms$)] + 6.6\% \times exp[t/(3$ ms$)]$). The not single-exponential behaviour can be accounted for the local magnetic moments of the first-row transition metal ions. The effect is more expressed with the increased effective magnetic moment. That is why only the manganese sample with the largest magnetic moment had two-exponential relaxation at the lower measuring frequency while at the higher frequency even the copper sample had non-exponential behaviour.

Table 3. Effective spin-spin relaxation times and ^1H spin-lattice relaxation times of $TM_2[Mo(CN)_8]\cdot nH_2O$

| TM | $v_0 = 27.694$ MHz | | $v_0 = 82.556$ MHz | | | | |
	T_{2eff} (μs)	T_1 (ms)	T_{2eff} (μs)	T_{1a} (ms)	f_a	T_{1b} (ms)	f_b
Cu	155.9	0.45	80.5	0.680	97 %	7.00	3 %
Ni	54.6	0.33	23.6	0.102	94 %	1.50	6 %
Co	39.2	1.1	12.3	0.020	13 %	1.26	87 %
Fe	30.3	0.156	10.1	0.018	50 %	0.21	50 %
Mn	12.8	0.0187	5.5	0.016	93 %	0.50	7 %
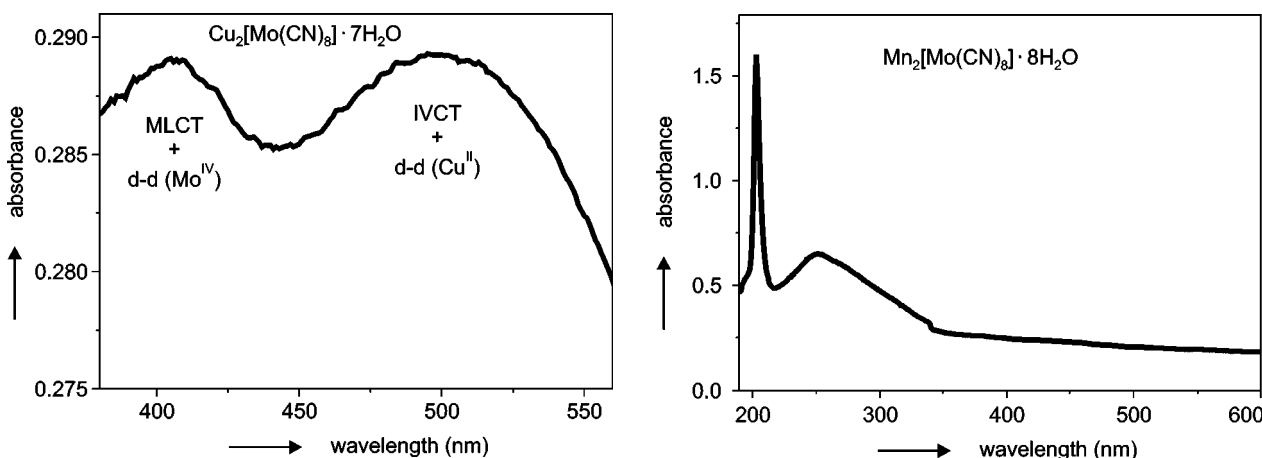
Figure 4. Absorbance UV-VIS spetra of $Cu_2[Mo(CN)_8]\cdot 7H_2O$ (left) and $Mn_2[Mo(CN)_8]\cdot 8H_2O$ (right), where MLCT is metal ligand charge transfer.

Magnetic measurements

The $\chi T(T)$ plots shown in figure 7(a) were measured in magnetic field $\mu_0 H = 1$ T. The sharp decrease of $\chi T(T)$ below $T = 30$ K can indicate onset of antiferromagnetic exchange interaction. In the case of Co²⁺ phase, $\chi T(T)$ decreases in the entire temperature range. Such a decrease of $\chi T(T)$ with T can be attributed to the intrinsic behaviour of Co²⁺ ion rather than to antiferromagnetic exchange interactions among these ions in the
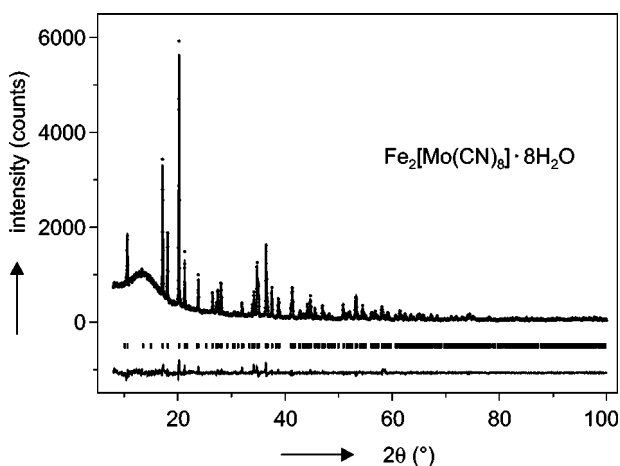
3D network. The samples obey the Curie-Weiss law $\chi = C/(T - \theta)$ nearly in the whole measured temperature range except of Co²⁺ sample, where $1/\chi(T)$ decreases remarkably below $T = 50$ K [22]. The paramagnetic Curie temperature is negative for Mn²⁺, Fe²⁺, Co²⁺ samples ($\theta = -1.3$ K, -3.1 K, -25.6 K) and close to zero for Ni²⁺, Cu²⁺ samples ($\theta = 0.0$ K, 0.3 K). We tried to determine the Curie temperature by several different methods. The classical method for obtaining the Curie temperature T_C by plotting M^2 vs. T and extrapolating the linear part to the temperature axis (Weiss method) gave the values, which varies in the range 3 K $< T_c < 4$ K for TM is Mn, Fe, and Co. On the other hand, the method of determining T_C by plotting $H/M(H,T)$ vs. $M^2(H,T)$ (Belov-Arrott's plots) gave the value of $T_C = 4$ K only in the case of Mn²⁺ and Co²⁺ containing samples. A ferromagnetic-like behaviour is seen also in the M(H,T) vs. H curves of Fe₂[Mo(CN)₈]·8H₂O. However, the fact that the Curie temperature could not be defined by using the Belov-Arrott method leads to the conclusion that there is only a short-range ordering in this sample in the vicinity of $T = 2$ K. Remaining complexes with Ni²⁺ and Cu²⁺ are paramagnetic in the whole temperature range. The results of the magnetic isotherms show that the magnetization is proportional to the magnetic field at higher temperatures and tends to saturate at very low temperatures and at higher magnetic fields (TM is Mn and Co). Magnetization curves of Mn₂[Mo(CN)₈]·8H₂O shown in figure 7b confirm the gradual development of magnetically ordered state in Mn²⁺ sample with magne-

Figure 5. The Rietveld refinement plot of the crystal structure of Fe₂[Mo(CN)₈]·8H₂O. The observed data are indicated by + symbols and the calculated ones by the solid line which overlay them. The positions of Bragg reflexions (for $\lambda = 1.54184$) are indicated by vertical markers.

a)

b)
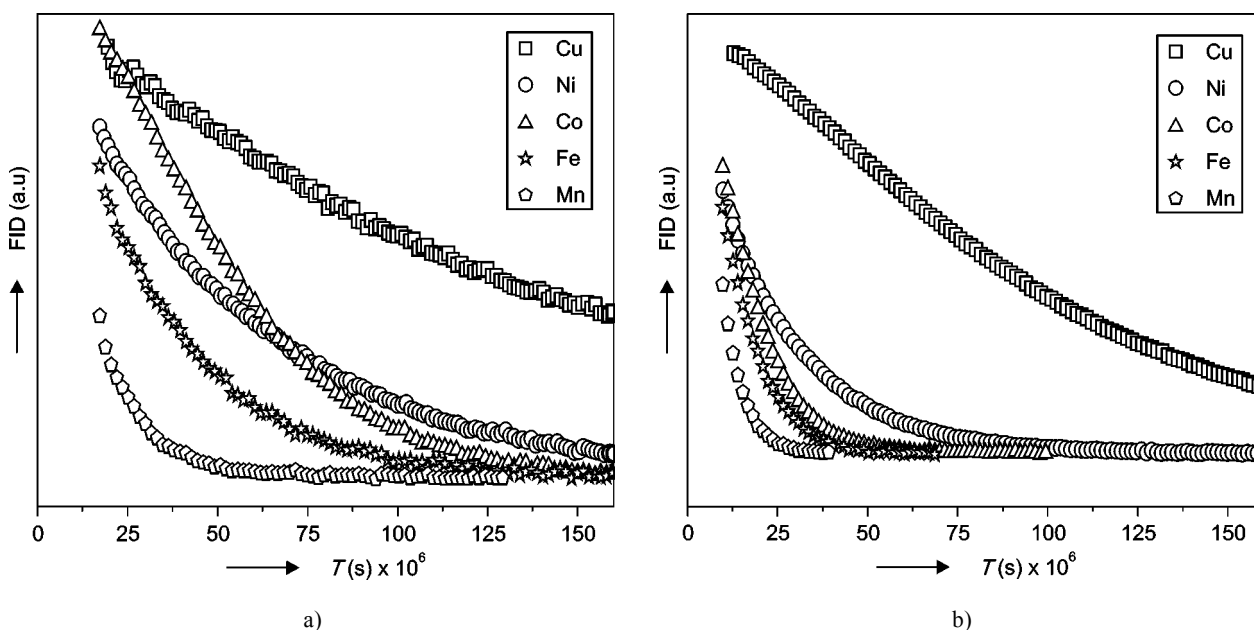
Figure 6. ¹H FID signals of TM₂[Mo(CN)₈]·nH₂O detected at (a) $\nu_0 = 27.694$ MHz and (b) $\nu_0 = 82.556$ MHz. FID amplitudes are normalized to unit mass of the samples.

tization reaching the value of $\mu_S = 8.2$ μ_B/f.u. at $T = 1.9$ K. Simi-lar behaviour we have observed for $Co_2[Mo(CN)_8]\cdot6H_2O$ with magnetization $\mu_S = 3.95$ μ_B/f.u.

The magnetic ordering of $TM^{2+}_2[Mo^{IV}(CN)_8]\cdot nH_2O$ octacyanometallates (TM is Mn, Fe, Co, Ni and Cu) is driven by the antiferromagnetic interaction between paramagnetic TM^{2+} ions through the NC–Mo^{IV}–CN diamagnetic spacer. The value of the exchange interaction is very weak due to contribution of diamagnetic Mo^{IV} resulting in the low value of the Curie temperature. The analysis of our magnetization measurements revealed that only $Mn_2[Mo(CN)_8]\cdot8H_2O$ and $Co_2[Mo(CN)_8]\cdot6H_2O$ show long range magnetic ordering of ferrimagnetic type below $T_C = 4$ K and a short range ordering starts to form in $Fe_2[Mo(CN)_8]\cdot8H_2O$ at about $T = 2$ K. Our results are consistent with results already published on Mn, Fe, and Cu OCMs [18, 19, 23]; to our knowledge, the results on Co and Ni OCMs have not been presented by another authors yet.

ture (space group *I4/mcm* and *I422*) with values of lattice parameters $a = 11.679(4)$ Å, $c = 13.205(6)$ Å, and $a = 11.80321(15)$ Å, $c = 13.1008(2)$ Å, respectively. Profile matching procedure confirmed the tetragonal symmetry for $Ni_2[Mo(CN)_8]\cdot8H_2O$ with lattice parameters $a = 11.555(4)$ Å and $c = 14.044(6)$ Å. The indexing procedure failed for $Cu_2[Mo(CN)_8]\cdot7H_2O$ due to poor crystallinity of the sample. The ^1H NMR signals reflect the magnetic moment of the TM^{2+} ions (μ_P). The decay rates of FID signals increase as μ_P and the applied static *rf*-field increases. The spin-lattice relaxation times at 27.7 MHz vary from 0.0187 ms (Mn) up to 0.45 ms (Cu). Magnetic behaviour of the investigated OCMs is determined by the electronic structure of the TM^{2+} ion and by the antiferromagnetic interaction between TM^{2+} ions through the NC–Mo^{IV}–CN diamagnetic spacer. Magnetization measurements indicate long-range magnetic ordering in Mn- and Co-OCMs with the Curie temperature about $T_c = 4$ K. The remaining OCMs (TM is Fe, Ni and Cu) are paramagnetic at least down to $T = 1.9$ K.

CONCLUSIONS

Cyano-bridged complexes $TM^{2+}_2[Mo(CN)_8]\cdot nH_2O$, where TM is Mn, Fe, Co, Ni, Cu were synthesised, characterised by IR spectroscopy and UV-VIS spectroscopy. The UV-VIS spectrum taken on the $Cu_2[Mo(CN)_8]\cdot7H_2O$ showed the (IVCT) between Mo^{IV}–CN–Cu^{II} and Mo^V–CN–Cu^I at around 510 nm. The amount of water in structural formulae n varies between 6 and 8. The Rietveld refinement showed that $Mn_2[Mo(CN)_8]\cdot8H_2O$ and $Fe_2[Mo(CN)_8]\cdot8H_2O$ adopt tetragonal crystal struc-
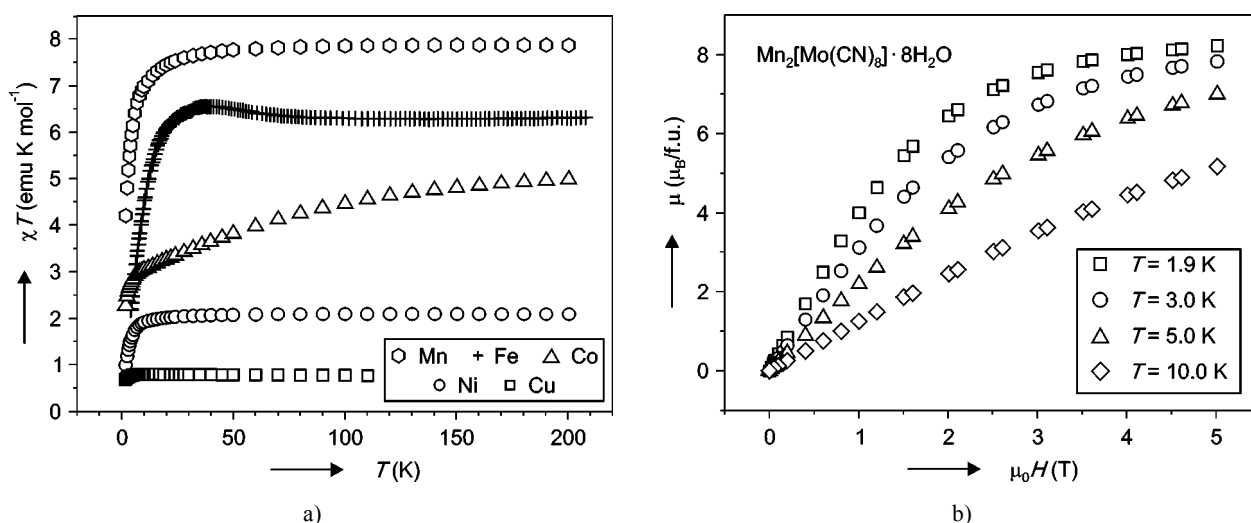
Figure 7. Magnetization curves of $TM_2[Mo(CN)_8]\cdot nH_2O$ (a) and of $Mn_2[Mo(CN)_8]\cdot8H_2O$ at different T (b).

References

1. Mallah T., Thiébaut S., Verdaguer M., Veilet P.: Science *1554*, 262 (1993).
2. Holmes S. M., Girolami G. S.: J.Am.Chem.Soc. *5593*, 121 (1999).
3. Verdaguer M.at all.: Coord.Chem.Rev. *190*, 1023 (1999).
4. Zhong, H. Seino Z. J., Mizobe Y., Midai M., Verdaguer M., Ohkoshi S. I., Hashimoto K.: Inorg.Chem. *39*, 5095 (2000).
5. Ohkoshi S. I.., Hashimoto K.: J.Photochem.Photobiol. C, *71*, 2 (2001)
6. Podgajny R., Desplanches C., Sieklucka B., Sessoli R., Villar V., Paulsen C.,. Wernsdorfer W, Dromzee Y., Verdaguer M.: Inorg.Chem. *41*, 1323 (2002).
7. Korzeniak T., Podgajny R., Alcock N. W., Lewinski K., Balanda M., Wasiutynski T., Sieklucka B.: Polyhedron *22*, 2183 (2003).
8. Sato O., Iyoda T., Fujishima A., Hashimoto K.: Science *49*, 271 (1996)
9. Sato O., Iyoda T., Fujishima A., Hashimoto K.: Science *272*, 704 (1996).
10. Ohkoshi S., Machida N., Zhong Z. J., Hashimoto K.: Synth. Met. *122*, 523 (2001).
11. Brauer G.: *Handbuch der Präparativen Anorganischen Chemie*, p.1653-1654, Ferdinand Enke Verlag, Stuttgart 1981.
12. Rodriguez-Carvajal J. in: Abstracts of the Satellite Meeting on Powder Diffraction of the XV Congress of the IUCr, p.127, Toulouse 1990.
13. Kettle S. F. A., Parish R. V.: Spectrochimica Acta *1087*, 21 (1965).
14. Hoard J. L., Nordsieck H. H.: J.Am.Chem.Soc. *2853*, 61 (1939).
15. Hendrickx M. F. A., Mironov V. S., Chibotaru L. F., Ceulemans A.: Inorg.Chem. *43*, 3142 (2004).
16. Rombaut G.: PhD thesis, University of Bordeaux France (2001)
17. Hennig H., Rehorek A., Rehorek D., Thomas Ph.: Inorg.Chim.Acta *41*, 86 (1984).
18. Sra A. K., Rombaut G., Lahitete F., Golhen S., Ouahab L., Mathoniere C., Yakhmi J. V., Kahn O.: New J.Chem. *24*, 871 (2000).
19. Rombaut G., Golhen S., Ouahab L., Mathoniere C., Khan O.: Inorg.Chem. *40*, 1151 (2001).
20. Willemin S., Larionova J., Clérac R., Donnadieu B., Henner B., Fréderic X., Guerin Ch.: Eur.J.Inorg.Chem. *1866* (2003).
21. Tuna F., Golhen S., Ouahab L., Sutter J.P.: C.R.Chimie *377*, 6 (2003)
22. Sendek M., Zentko A., Mihalik M., Zentková M., Mitróová Z., Kavečanský V., Bokor M., Maryško M.: Czech.J.Phys *54*, D551 (2004).
23. Rombaut G., Mathoniere C., Guionneau P., Golhen S., Ouahab L., Verelst M., Lecante P.: Inorg.Chim.Acta, *326*, 27 (2001).

SYNTÉZA, STRUKTURA A MAGNETICKÉ
VLASTNOSTI TM²⁺₂[Moᴵⱽ(CN)₈].nH₂O

ZUZANA MITRÓOVÁ, MARIÁN MIHALIK,
ANTON ZENTKO, MÓNIKA BOKOR*,
KATALIN KAMARÁS*,
VIKTOR KAVEČANSKÝ, JOZEF KOVÁČ,
KORNEL CSACH, JARMILA TRPČEVSKÁ**

*Ústav experimentální fyziky SAV,
Watsonova 47, 043 53 Košice, Slovensko
*Research Institute for Solid State Physics and Optics
of the Hungarian Academy of Science,
P.O. Box 49, H-1525 Budapest, Hungary
**Technická Univerzita Košice,
Letná 9, 042 00 Košice, Slovensko*

Oktakyanomolybdeničitany (OCM) TM²⁺₂[Mo(CN)₈].nH₂O, kde TM je Mn, Fe, Co, Ni, Cu, byly syntetizovány a charakterizovány IČ a UV-VIS spektroskopií. V UV-VIS spektru jsou patrné pásy intervalenčního přenosu náboje (IVCT) mezi Moᴵⱽ-CN-Cuᴵᴵ a Moⱽ-CN-Cuᴵ kolem 510 nm. Studované OCM mají tetragonální krystalovou strukturu. ¹H NMR signál ukazuje na magnetický moment iontů TM²⁺ (μ_P). Rychlost poklesu volného indukovaného rozkladu (FID) signálu roste s poklesem μ_P a vloženého statického *rf*-pole. Spinově-mřížkové relaxační časy při 27.7 MHz kolísají mezi 0.0187 ms (Mn) až 0.45 ms (Cu). Měření magnetizace svědčí o magnetickém uspořádání na dlouhou vzdálenost v OCM s Mn a Co s Curieovou teplotou T_c = 4 K. Ostatní OCM (TM je Fe, Ni, Cu) jsou paramagnetické až do T = 1.9 K.